

Percolation Metal-Insulator Transitions in the Two-Dimensional Electron System of AlGaAs/GaAs Heterostructures

A. A. Shashkin, V. T. Dolgoplov, and G. V. Kravchenko

Institute of Solid State Physics, Chernogolovka, 142432 Moscow District, Russia

M. Wendel, R. Schuster, and J. P. Kotthaus

Ludwig-Maximilians-Universität, Geschwister-Scholl-Platz 1, 80539 München, Germany

R. J. Haug, K. von Klitzing, and K. Ploog

Max-Planck-Institut für Festkörperforschung, 70569 Stuttgart, Germany

H. Nickel and W. Schlapp

Telekom Forschungs- und Technologiezentrum, 64295 Darmstadt, Germany

(Received 23 May 1994)

We investigate the transport properties of insulating phases in the 2D electron system of high-mobility AlGaAs/GaAs heterostructures of Corbino geometry at very low temperatures. We find that the nonlinear current-voltage characteristics for insulating phases in the integer and fractional quantum Hall regime and for a low-density insulating phase are very similar. The behavior of these characteristics with changing temperature and filling factor unambiguously points to the percolation metal-insulator transition as the cause for all insulating phases investigated. We propose a metal-insulator phase diagram in the (B, N_s) plane based on our experimental data.

PACS numbers: 71.30.+h, 73.20.Dx, 73.40.Kp

The metal-insulator transition at low filling factors in a 2D electron system of high-mobility AlGaAs/GaAs heterostructures has been investigated in a number of studies (see, e.g., [1–5]) by using various experimental techniques. In the majority of the reports the transition into an insulating phase is attributed to the formation of a pinned Wigner crystal. However, some doubts in this interpretation were expressed, e.g., in Ref. [6]. Optical investigations strongly suggest that in high magnetic fields the 2D electron system becomes strongly inhomogeneous; in photoluminescence spectra there coexist two lines, one of which is caused by radiative recombination of 2D electrons from metallic regions [4,7,8] and the other proves the existence of insulating islands in the electron system. The conduction of an inhomogeneous macroscopic system is determined by the coverage of the sample with metallic and insulating areas, respectively. In this case the metal-insulator transition must be discussed as a percolation problem. Here we introduce a method based on investigations of the current-voltage characteristics which makes it possible to compare the transport properties of insulating phases realized in the integer and fractional quantum Hall regime and at low electron densities in AlGaAs/GaAs heterostructure samples. Our experimental results provide strong evidence for the percolation nature of all metal-insulator transitions studied.

Let us first consider the definition of insulating phases in a 2D system. As known, in the integer and fractional quantum Hall regime the Hall conductivity σ_{xy} is quantized and the dissipative conductivity σ_{xx} tends to zero

at low temperatures. The Hall conductivity is finite due to the existence of extended states below the Fermi level that are able to carry dissipationless Hall current, as has been shown in experiments on charge transfer in Corbino samples [9]. It is reasonable to call such a state of the 2D electron system an insulator because the Fermi level lies in localized states and electron transport in the direction of the electric field is absent. Obviously, a so-defined insulating phase can be characterized by the value of the Hall conductivity. The insulating phase at low electron densities corresponds to $\sigma_{xy} = 0$ since in this case the extended states below the Fermi level are not available [10] so that both the conductivities σ_{xx} and σ_{xy} vanish at low temperatures.

In our experiments we use Corbino samples made of two AlGaAs/GaAs wafers (*A* and *B*) with mobility $\mu \approx 10^6$ cm²/Vs. The spacer layer thickness of these wafers is 700 and 300 Å, and the inner and outer radii of the Corbino rings are $r_1 = 1.0$ mm, $r_2 = 1.02$ mm and $r_1 = 0.2$ mm, $r_2 = 0.5$ mm, respectively. In the latter case the samples have a circular gate restricted by radii $r_{1g} = 0.3$ mm and $r_{2g} = 0.4$ mm so that a gated region of 2D layer is separated from the contacts by guarding rings. Applying a dc voltage between the gate and one of the contacts, we control the electron density in the gated region while in the guarding rings it remains unchanged. On these samples experiments are carried out at different electron densities, but only in the ranges of a magnetic field where the conductivity σ_{xx} in the ungated region is metallic.

We study current-voltage characteristics of an insulating phase at very low densities as well as of the insulating phases in the fractional and integer quantum Hall regime corresponding to filling factors $\nu = 2/3, 1, 2$. Measurements were made by a dc technique in the temperature range 25 mK to 0.5 K and at magnetic fields of up to 16.5 T. We determine from I - V characteristics at lowest temperature where the nonlinearities are most pronounced a threshold voltage U_c that is defined according to the inset in Fig. 1. The temperature dependence of the resistance in the linear part of the I - V characteristics yields an activation energy E_a . The method we propose is based on the fact that the behavior of the threshold voltage and activation energy as a function of filling factor at the metal-insulator transition allows us to establish the nature of this transition and thereby to discriminate between the possible origins of the insulating phases.

Typical current-voltage characteristics for the insulating phase with $\sigma_{xy}h/e^2 = 2/3$ are presented in the inset of Fig. 1. As seen from the figure, at a minimum temperature the initial linear rise of the voltage with current strongly slows at some threshold voltage U_c . (Some authors define two critical voltages, one of which corresponds to the onset of weak nonlinearities and the other characterizes the strongly nonlinear regime [3,6,11,12].) Such a behavior of I - V characteristics is observed in all insulating phases, while in the metallic phase the I - V characteristics are linear in the whole range of currents used. As the temperature increases the nonlinearities are smeared out (inset in Fig. 1): At lowest temperatures the resistance in the linear interval of I - V characteristics obeys the variable range-hopping law while at higher temperatures the resistance shows an activated temperature dependence (see inset in Fig. 2). Owing to

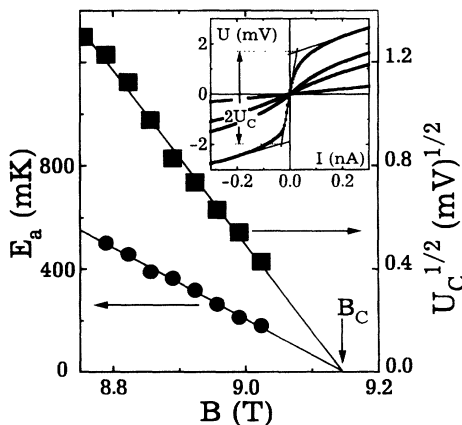


FIG. 1. Activation energy and square root of the critical voltage U_c as a function of magnetic field for the $2/3$ quantum Hall state. Wafer A. Typical current-voltage characteristics are shown in the inset at $B = 8.76$ T and $T \approx 25$ mK, 60 mK, 74 mK, and 114 mK. The size of points in all figures corresponds to the experimental uncertainty.

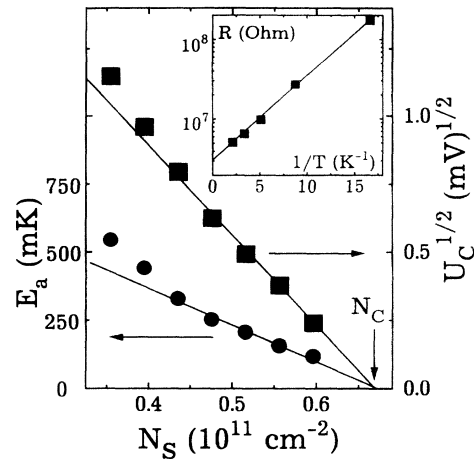


FIG. 2. Behavior of the activation energy and the critical voltage for the low-density insulating phase. $B = 16.5$ T; wafer B. Inset: Arrhenius plot of the resistance in the linear regime at $B = 16.5$ T, $N_s = 4.8 \times 10^{10}$ cm $^{-2}$. The value of the resistance is normalized by aspect ratio.

the growth of the resistance in the linear regime, the shape of the I - V characteristics for the insulating phase tends to a steplike function both with decreasing temperature and when departing from the phase boundary. That is why we can observe far more pronounced nonlinearities in the phases with $\sigma_{xy}h/e^2 = 0, 1, 2$, as compared to those in the $2/3$ insulating phase.

Surprisingly, we find that the behavior of both the threshold voltage and activation energy is the same for all insulating phases investigated: The dependences of $U_c^{1/2}$ and E_a on magnetic field (or electron density) are linear and run to the same point B_c (or N_c) corresponding to the mobility edge E_c (see, e.g., Figs. 1 and 2); i.e., both of the values tend to zero as the metal-insulator phase boundary is approached. We have tested the validity of these statements at the phase boundary points indicated in Fig. 3. Thus, from our experiments follows that a critical electric field F_c corresponding to U_c is written as

$$F_c = \beta E_a^2. \quad (1)$$

The measured values of the coefficient β at different phase boundaries on the same sample are found to coincide within experimental uncertainty.

In the case of insulating phases in the integer quantum Hall regime, we can easily interpret the relation (1) in terms of the percolation picture [13,14]. (Evidently, the linear change of the activation energy with filling factor is determined by the value of density of states near E_c . The deviation of E_a and $U_c^{1/2}$ from the linear dependences in Fig. 2 is due to the drop of the density of states as the absolute value of $N_s - N_c$ increases.) At sufficiently low temperatures the conduction in the insulating phase is caused by variable range hopping, while in a cluster the electron system is metallic. In the vicinity of the mobility

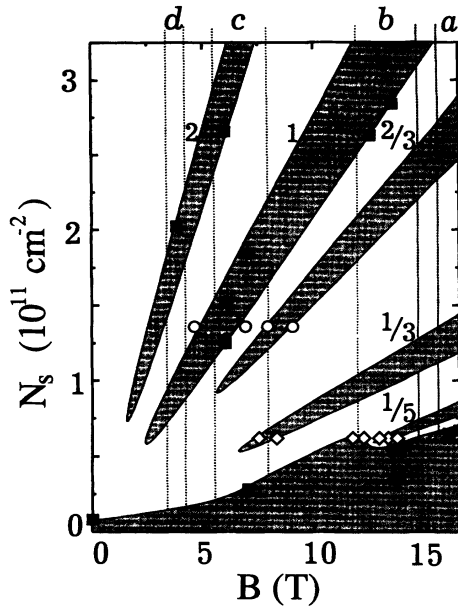


FIG. 3. Metal-insulator phase diagram in the (B, N_s) plane. The points corresponding to phase boundaries are obtained on different samples: \circ , wafer A; \blacksquare , wafer B; \diamond , we took this data from Ref. [11] regarding that at a minimum temperature the reciprocal of the conductivity σ_{xx} at mobility edge E_c is equal to 10 M Ω as follows from our results. The solid lines are guides to the eye. Vertical lines restrict the regions a, b, c , and d of a magnetic field for gated samples where σ_{xx} in the guarding rings was sufficiently high. Digits indicate the Hall conductivity in units e^2/h for different insulating phases.

edge the average cluster radius, or the localization length $L(E)$, is expected to diverge with the critical index s :

$$L(E) = \frac{1}{\beta^*} |E - E_c|^{-s}, \quad (2)$$

where β^* characterizes a random potential. At sufficiently low electric fields the clusters form equipotential areas so that the energy separation between the mobility edge E_c and the electron energy in a cluster decreases by $eFL(E_F)$. At the critical electric field F_c defined by the expression

$$F_c = \frac{E_a}{eL(E_F)} = \frac{\beta^*}{e} E_a^{s+1}, \quad (3)$$

the electrons reach the mobility edge, which gives rise to an abrupt increase of the conduction in agreement with the experiment. [We note that in such a model the energy $eF_cL(E_F)$ is equal to E_a and can considerably exceed the base electron temperature.] It is seen that Eqs. (1) and (3) are identical if $\beta^* = e\beta$ and the critical index $s = 1$, which is close to the theoretical value $s = 1.3$ expected for classical percolation. Hence, the breakdown of insulating phases can be explained by electric-field-induced electron delocalization in the classical percolation picture [15].

Indeed, we expect that at integer filling factors the properties of 2D electron systems should be similar as

long as the screening of random potential by electrons in totally occupied Landau levels is negligible. In the case of the fractional quantum Hall effect, the experimental results are surprising: the 2D electron system is found to have very similar properties in both the integer and fractional quantum Hall regime. Our results also show that the transition into the low-density insulating phase is the percolation one and occurs at $\nu_c \approx 0.17$. The percolation nature of the transition into the low-density insulating phase is confirmed, in our opinion, by data on the higher mobility samples where this transition was initially attributed to the formation of a pinned Wigner solid. Indeed, in Ref. [11] it was found that for the low-density insulating phase the imaginary part of the high-frequency conductivity diverges as $\text{Im}(\sigma_{xx}) \propto |B - B_c|^{-1}$. Since $\text{Im}(\sigma_{xx})$ is determined by the dielectric permeability of the system, which is proportional to the cluster dimension within a percolation picture, the results [11] are in agreement with our conclusions. We find additional confirmation in Ref. [7]. From time-resolved photoluminescence of 2D electrons, one can determine the metal-insulator transition point, assuming the percolation character of the transition. According to the percolation theory, the transition occurs at a magnetic field where the area of metallic regions is equal to half of the sample area. Assuming the integral intensity of radiative recombination from metallic regions to be proportional to their area, we obtain from data in Ref. [7] $\nu_c \approx 0.19$, which agrees with our observations. We note that in Ref. [7] insulating regions in the electron system were associated with the Wigner solid phase. If this were true, then the nonlinear I - V characteristics should be explained by crystal depinning. This starts when the work of the electric field to shift a crystallite with dimension d on the distance between electrons is equal to the activation energy $E_a = eF_c d^2 N_s^{1/2}$ (see, e.g., Refs. [16,17]). Hence, one could expect that near the phase transition F_c and E_a should be proportional to each other. However, this is not the case, as follows from our experiments. Therefore, we conclude that the origin of the low-density insulating phase is the localization of electrons in a random potential rather than the pinned Wigner crystal.

On the basis of our experimental results we propose a metal-insulator phase diagram in the (B, N_s) plane for high-mobility 2D electron systems (Fig. 3). (Phase diagrams for low-mobility systems were discussed in a number of experimental works [14,18–20].) The phase diagram is not universal in the sense that the exact position of boundaries changes for different samples. However, its topology is expected to be universal: each integer or fractional quantum Hall state corresponds to a hatched area indicating an insulating phase surrounded by the metallic phase. The nonmonotonic behavior of the lowest phase boundary reflects the so-called reentrant transition into the low-density insulating phase. The proposed phase diagram is in agreement with the results

obtained on Si metal-oxide-semiconductor field effect transistors (MOSFET's) [14,20] and similar, in principle, to the diagram discussed in recent theoretical studies [21].

One can expect that with improving sample quality the coefficient β should increase so that the dependence $L(E)$ given by Eq. (2) will ultimately tend to a δ function. Comparison of the values of β for different samples reveals the expected correlation: On wafer A ($\beta \approx 3$ V/cm K²) the fractions are more pronounced than on wafer B ($\beta \approx 0.7$ V/cm K²), while on Si MOSFET's ($\beta \approx 0.1$ V/cm K²) [14] they are not observed at $B < 16$ T. Hence, we can introduce the coefficient β , in addition to the mobility, as a characteristic of the sample. In contrast to the mobility determined in the metallic phase when potential fluctuations are well screened, the β value directly reflects properties of a random potential when the Fermi level lies within localized states and screening is less effective.

In summary, we have investigated the behavior of non-linear current-voltage characteristics for the low-density insulating phase of AlGaAs/GaAs heterostructures as well as for insulating phases in the integer and fractional quantum Hall regime. We find that near the metal-insulator transition the critical electric field F_c corresponding to the onset of nonlinearities is proportional to the square of the activation energy E_a of the resistance in the linear regime with the same coefficient β for all the insulating phases. Both F_c and E_a tend to zero as the metal-insulator phase boundary is approached. Comparison of the experimental data on different samples shows that the value of β correlates with the sample quality. These results point to the same origin of all insulating phases and can be interpreted in terms of the percolation picture in which the breakdown of the insulating phases is explained by electric-field-induced electron delocalization. Making use of our results, we propose the metal-insulator phase diagram in the (B, N_s) plane for the 2D electron system of AlGaAs/GaAs heterostructures.

We are thankful to Dr. W. Hansen for helpful discussions of the manuscript. This work was supported by Volkswagenstiftung under Grant No. I/68553 and, in part, by Grant No. 93-02-2304 from The Russian Foundation for Basic Research.

[1] E. Y. Andrei, G. Deville, D. C. Glattli, and F. I. B.

- Williams, Phys. Rev. Lett. **60**, 2765 (1988).
- [2] H. W. Jiang, R. L. Willett, H. L. Stormer, D. C. Tsui, L. N. Pfeiffer, and K. W. West, Phys. Rev. Lett. **65**, 633 (1990).
- [3] V. J. Goldman, M. Santos, M. Shayegan, and J. E. Cunningham, Phys. Rev. Lett. **65**, 2189 (1990).
- [4] H. Buhmann, W. Joss, K. von Klitzing, I. V. Kukushkin, A. S. Plaut, G. Martinez, K. Ploog, and V. B. Timofeev, Phys. Rev. Lett. **66**, 926 (1991).
- [5] G. M. Summers, R. J. Warburton, J. G. Michels, R. J. Nicholas, J. J. Harris, and C. T. Foxon, Phys. Rev. Lett. **70**, 2150 (1993).
- [6] H. W. Jiang, H. L. Stormer, D. C. Tsui, L. N. Pfeiffer, and K. W. West, Phys. Rev. B **44**, 8107 (1991).
- [7] I. V. Kukushkin and V. B. Timofeev, Usp. Fis. Nauk **163**, 1 (1993) [Sov. Phys. Usp. **36**, 549 (1993)].
- [8] S. A. Brown, A. G. Davies, A. C. Lindsay, R. B. Dunford, R. G. Clark, P. E. Simmonds, H. H. Voss, J. J. Harris, and C. T. Foxon, Workbook EP2DS-10, Newport, 1993, p. 636.
- [9] V. T. Dolgoplov, N. B. Zhitenev, and A. A. Shashkin, JETP Lett. **52**, 196 (1990); Europhys. Lett. **14**, 255 (1991); V. T. Dolgoplov, A. A. Shashkin, N. B. Zhitenev, S. I. Dorozhkin, and K. von Klitzing, Phys. Rev. B **46**, 12560 (1992).
- [10] V. T. Dolgoplov, A. A. Shashkin, G. V. Kravchenko, S. I. Dorozhkin, and K. von Klitzing, Phys. Rev. B **48**, 8480 (1993).
- [11] Y. P. Li, dissertation, Princeton University, 1994.
- [12] F. I. B. Williams, P. A. Wright, R. G. Clark, E. Y. Andrei, G. Devill, D. C. Glattli, O. Probst, B. Etienne, C. Dorin, C. T. Foxon, and J. J. Harris, Phys. Rev. Lett. **66**, 3285 (1991).
- [13] V. T. Dolgoplov, G. V. Kravchenko, A. A. Shashkin, and S. V. Kravchenko, Phys. Rev. B **46**, 13303 (1992).
- [14] A. A. Shashkin, V. T. Dolgoplov, and G. V. Kravchenko, Phys. Rev. B **49**, 14486 (1994).
- [15] A. A. Shashkin, A. J. Kent, P. A. Harrison, L. Eaves, and M. Henini, Phys. Rev. B **49**, 5379 (1994).
- [16] B. G. A. Normand, P. B. Littlewood, and A. J. Millis, Phys. Rev. B **46**, 3920 (1992).
- [17] X. Zhu, P. B. Littlewood, and A. J. Millis, Phys. Rev. Lett. **72**, 2255 (1994).
- [18] V. M. Pudalov, M. D'Iorio, S. V. Kravchenko, and J. W. Campbell, Phys. Rev. Lett. **70**, 1866 (1993).
- [19] H. W. Jiang, C. E. Johnson, K. L. Wang, and S. T. Hannahs, Phys. Rev. Lett. **71**, 1439 (1993).
- [20] A. A. Shashkin, G. V. Kravchenko, and V. T. Dolgoplov, JETP Lett. **58**, 220 (1993).
- [21] B. I. Halperin, P. A. Lee, and N. Read, Phys. Rev. B **47**, 7312 (1993).

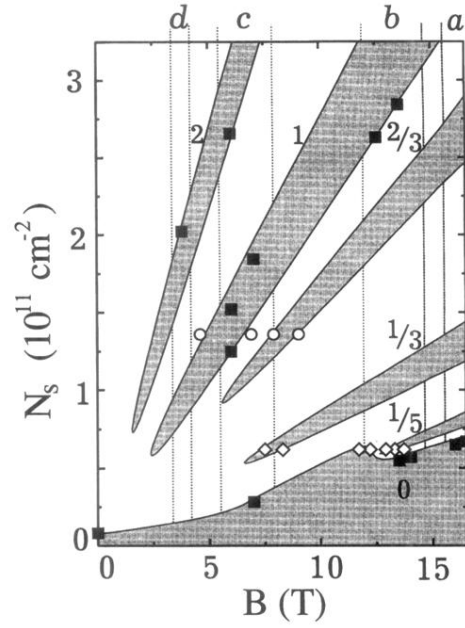


FIG. 3. Metal-insulator phase diagram in the (B, N_s) plane. The points corresponding to phase boundaries are obtained on different samples: \circ , wafer A; \blacksquare , wafer B; \diamond , we took this data from Ref. [11] regarding that at a minimum temperature the reciprocal of the conductivity σ_{xx} at mobility edge E_c is equal to $10 \text{ M}\Omega$ as follows from our results. The solid lines are guides to the eye. Vertical lines restrict the regions a, b, c , and d of a magnetic field for gated samples where σ_{xx} in the guarding rings was sufficiently high. Digits indicate the Hall conductivity in units e^2/h for different insulating phases.